Hydrodynamics Versus Intracellular Coupling in the Synchronization of Eukaryotic Flagella

Greta Quaranta,[1] Marie-Eve Aubin-Tam,[2,*] and Daniel Tam[1,†]
[1]*Laboratory for Aero and Hydrodynamics, Delft University of Technology, 2628CD Delft, Netherlands*
[2]*Department of Bionanoscience, Delft University of Technology, 2628CJ Delft, Netherlands*
(Received 30 June 2015; published 30 November 2015)

The influence of hydrodynamic forces on eukaryotic flagella synchronization is investigated by triggering phase locking between a controlled external flow and the flagella of *C. reinhardtii*. Hydrodynamic forces required for synchronization are over an order of magnitude larger than hydrodynamic forces experienced in physiological conditions. Our results suggest that synchronization is due instead to coupling through cell internal fibers connecting the flagella. This conclusion is confirmed by observations of the *vfl3* mutant, with impaired mechanical connection between the flagella.

DOI: 10.1103/PhysRevLett.115.238101 PACS numbers: 87.16.Qp, 05.45.Xt, 47.63.Gd

The emergence of coherent behavior is ubiquitous in the natural world and has long captivated physicists and biologists alike [1]. Phase transitions leading to synchronization are observed between and within a variety of biological organisms [2]. Recently, the organized dynamics of micron sized hairlike cell projections called eukaryotic flagella or cilia has attracted high levels of interest [3–5]. The ability of flagella to manipulate and transport fluid relies on their capacity to spontaneously beat and synchronize with one another. Identifying the physical mechanisms leading to flagellar synchronization has been the subject of intense investigations in recent years [6,7].

Theoretical studies on flagellar synchronization in the inertialess viscous regime began with work by Taylor [8], which highlighted the role of hydrodynamics. Experimental work has focused on a model organism for motility: unicellular green alga *Chlamydomonas reinhardtii*. *C. reinhardtii* possesses two flagella, the *cis* and the *trans* flagellum, which beat in synchrony for long time periods [7,9–11]. Flagella have often been suggested to synchronize due to interflagellar hydrodynamic interactions. This view has been supported by several theoretical studies [3,4,12,13] and recent experiments [14,15]. Recently, another view has emerged, suggesting that the cell rocking motion causes synchronization by creating synchrony-restoring hydrodynamic drag on the flagella [16,17].

Both mechanisms imply that synchronization is mediated by hydrodynamic forces. To what extent flagella respond to hydrodynamic forces remains undetermined. Here, we develop an experimental approach to actively interact with *C. reinhardtii*. Controlled hydrodynamic forces are applied on the cell by generating external periodic background flows. Controlled perturbations have been imposed on biological systems in previous investigations of hair cells and flagella [14,18–20]. Our experiments reveal that flagellar beating can be controlled solely *via* hydrodynamic forces generated by an external periodic flow. However, we find the hydrodynamic forces required for synchronization to be over an order of magnitude larger than the forces experienced by the cell in physiological conditions and, hence, unlikely to be relevant to synchronization in *C. reinhardtii*. Our results suggest instead that coupling occurs through the cell-internal fiber connecting the flagella. The potential role of such fibers in the synchronized behavior of *C. reinhardtii* remains unclear. These cell-internal fibers have been hypothesized to determine and modulate the flagella beating mode [9,21] and have also been suggested to provide the mechanical connection at the origin of synchronization itself [22–24]. This last hypothesis is corroborated by our experimental observations of the *vfl3* mutant, with impaired mechanical connection between the flagella.

Experimental approach.—Wild-type (wt) *C. reinhardtii* (strain CC125) is grown in Tris-minimal medium [25] with sterile air bubbling, and subject to light:dark (14:10 h) cycles with light intensity of 230 $\mu\mathrm{E}\cdot\mathrm{m}^{-2}\cdot\mathrm{s}^{-1}$. When culture density reaches 10^6 cells $\cdot\,\mathrm{ml}^{-1}$, the suspension is diluted in Tris media. *C. reinhardtii* mutant *vfl3* (strain CC1686) is grown similarly in TAP medium [25]. A custom-made flow chamber of height $h = 1.5$ mm, with a 15×1.5 mm rectangular opening on one side, is filled with the diluted cell suspension until the air-water interface is pinned on all edges of the opening. The flow chamber is placed on a piezoelectric stage (Nano-Drive, Mad City Labs) under an inverted microscope with a 60× water-immersion objective. A micropipette is inserted inside the chamber, without direct contact with the chamber. A single cell is captured at the tip of the micropipette; see Fig. 1. When the stage position $X(t)$ varies, the cell remains fixed in the laboratory frame of reference. We impose $X(t)$ as a triangular wave of amplitude A_F and frequency f_F. The motion of the piezo is calibrated in separate experiments by tracking microbeads. The flow velocity field is measured

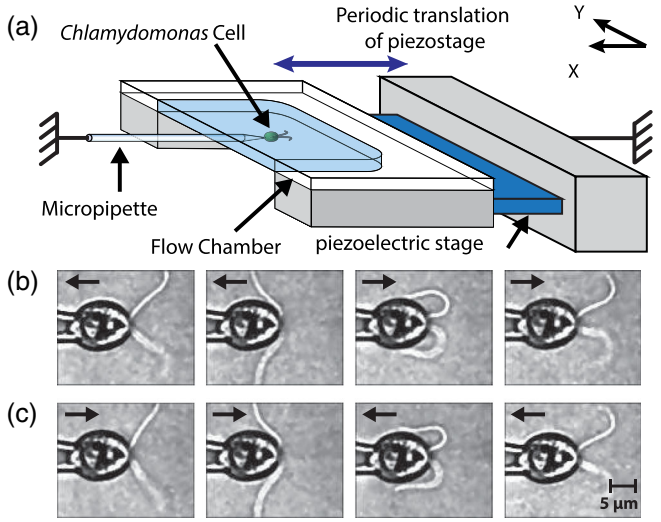

FIG. 1 (color online). (a) Experimental setup. (b) Snapshots representing the stroke patterns of *C. reinhardtii*, for a cell with $f_0 = 54.3$ Hz and an external flow with $f_F = 52.7$ Hz and $U_F = \pm 527$ μm.s^{-1}. Time between snapshots: 6 ms. Arrows represent the direction of the background flow. In this sequence, the flagella beat with the flow and the flagellar tip motion has the same direction as the external flow. (c) Snapshots of same cell as in (b) 0.33 s later. The flagella beat against the flow.

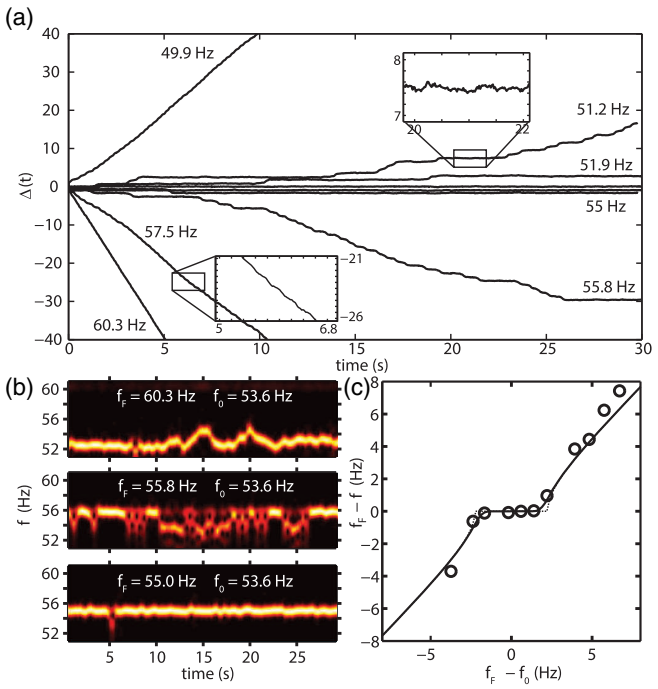

FIG. 2 (color online). Experimental data for one data set. The same cell is subject to an external flow $A_F = 5$ μm and $f_F = 49.9$–60.3 Hz. (a) Time variations of the phase difference between the flagella and the external flow for separate recordings. Inset for $f_F = 57.5$ Hz shows a stepwise decay of $\Delta(t)$. Inset for $f_F = 51.2$ Hz shows fluctuations during phase locking. (b) Spectrograms of flagellar motion for different f_F. Black (white) correspond to a low (high) amplitude in the frequency spectrum. From top: no synchrony ($f_F = 60.3$ Hz), partial locking ($f_F = 55.8$ Hz), and complete phase locking ($f_F = 55.0$ Hz). (c) $f_F - f$ as a function of $f_F - f_0$: Symbols, experimental data; solid line, f is computed from Eq. (4) with the fitted values for f_0, ϵ_0, and T_{eff}; dotted line, f is computed from Eq. (4) in the limit of zero noise.

inside the chamber around the micropipette and compared with numerical computations of the velocity field around a micropipette; see Supplemental Material [26]. We find the motion of the stage to induce a unidirectional periodic background flow around the cell with constant velocity $U(t) = \pm U_F = \pm 2A_F f_F$ corresponding to a constant periodic forcing.

Flagella motion is recorded under bright field illumination of light intensity 160 μE $\cdot$ m^{-2} $\cdot$ s^{-1} with a sCMOS camera (PCO.edge 5.5) at 838.4 fps. Movies are processed to track the passage of each flagellum through an interrogation window [7,14]. From this procedure, we deduce the phase dynamics of both the *cis* and the *trans* flagellum and the time variations of the frequency spectrum, which we represent in spectrograms; see Fig. 2(b) [31]. The phase dynamics of the two flagella are nearly identical, with few interflagellar slips recorded. We hence consider $\phi(t)$ to represent the phase of both beating flagella and deduce the time-dependent phase difference $\Delta(t)$ between the flagella and the external forcing flow $\Delta(t) = \phi(t) - \phi_F(t)/2\pi$, where $\phi_F(t) = 2\pi f_F t$.

Experimental observations.—A cell is subject to a series of different flow conditions. The flow amplitude A_F remains constant while the flow frequency f_F is varied incrementally. Recordings in the absence of flow are taken at regular intervals to determine the intrinsic beating frequency of the cell f_0 and monitor motility. Figures 2 and 3 present experimental results for one particular cell with $f_0 = 53.6 \pm 0.7$ Hz. This cell is subject to background flows of $A_F = 5$ μm and flow frequencies 49.9–60.3 Hz, corresponding to flow velocities $U_F = 499$–603 μm $\cdot$ s^{-1}. For $f_F = 57.5$–60.3 Hz, higher than the intrinsic frequency, the phase difference $\Delta(t)$ decreases uniformly with time and the flagella do not synchronize with the background flow, Fig. 2(a). The beating frequency f remains close to f_0 and does not lock with f_F throughout the 30 s of recording. Fluctuations around f_0 are observed in the beating frequency [32] [Fig. 2(b), top]. The power and recovery strokes are weakly affected by the direction of the flow and flagellar strokes remain well defined regardless of whether the cell beats with [Fig. 1(b)] or against the flow [Fig. 1(c)]. For the lower value $f_F = 57.5$ Hz, $\Delta(t)$ decreases in stepwise fashion, signifying the proximity of a synchronization transition; see inset in Fig. 2(a). At $f_F = 55.8$ Hz, $\Delta(t)$ is archetypical of a synchronization transition for a noisy oscillator [33]. Periods of phase locking of duration up to 4 s are interrupted by periods over which $\Delta(t)$ decreases as $\phi(t)$ progressively slips compared to $\phi_F(t)$, Fig. 2(a). When the phases are locked, $f = f_F$, while $f = f_0$ otherwise

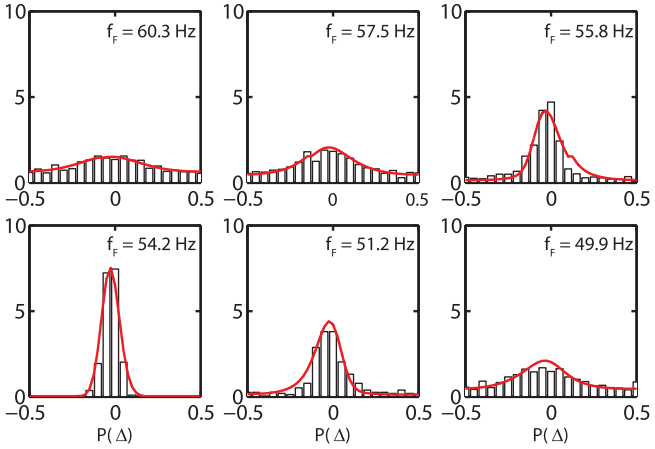

FIG. 3 (color online). Histograms showing the distributions of phase difference $\Delta(t)$ in separate recordings of the same cell, with external flows at $A_F = 5$ μm and different f_F. Red line: $\hat{P}(\Delta)$ computed with the fitted parameters $f_0 = 53.6$ Hz, $\epsilon_0/f_0 = 0.042$, and $T_{\text{eff}}/f_0 = 0.0006$.

[Fig. 2(b), center]. For $f_F = 53.4$–55 Hz, the phases remain locked for the entire 30 s of each recordings in a 1:1 in-phase locking mode with $f = f_F$ [Fig. 2(b), bottom]. Few occasional phase slips are observed at $f_F = 51.9$ Hz, when the cell performs one additional beat and Δ rapidly increases by one unit. Finally, as f_F is further decreased, the reverse transition to asynchronous behavior takes place. Our observations are consistent with the behavior of a self-sustained periodic oscillator under periodic external action in the presence of small bounded noise [33]. The same experiments were performed with the background flow in the direction perpendicular to the pipette axis. In these experiments, phase-locking was rarely triggered for such transverse flows.

Synchronization regions.—We proceed by determining the hydrodynamic forces required to control flagellar motility and achieve phase locking. We do so by fitting our data to a low-order model for the synchronization of an oscillator with an external forcing. The stochastic fluctuations of the phase difference $\Delta(t)$ are modeled as a Langevin dynamics

$$\frac{d\Delta(t)}{dt} = -\frac{dV(\Delta)}{d\Delta} + \xi(t), \tag{1}$$

where $\xi(t)$ represents a random noise in the flagellar actuation and $V(\Delta)$ is the potential associated with the deterministic force driving $\Delta(t)$. With $-dV(\Delta)/d\Delta = -\nu - \epsilon \sin[2\pi\Delta(t)]$, Eq. (1) yields the stochastic Adler equation, where $\nu = f_F - f_0$ is the detuning parameter and ϵ the coupling strength between the flagella and the external flow [33]. We assume $\xi(t)$ to be a Delta-correlated Gaussian noise of intensity T_{eff}, such that $\langle \xi(\tau)\xi(\tau + t)\rangle = 2T_{\text{eff}}\Delta(t)$. From Eq. (1), one can derive a Fokker-Planck equation for the probability density function $P(\Delta, t)$:

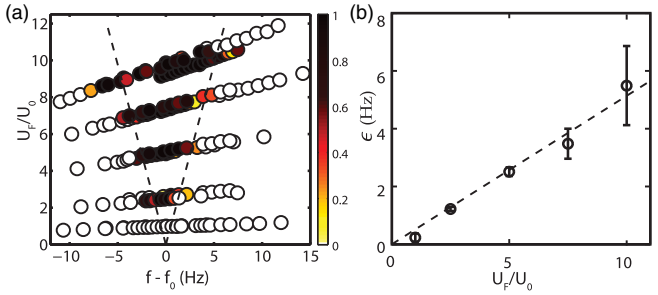

FIG. 4 (color online). (a) Synchronization region in (f_F, U_F) domain. Each marker represents a separate recording. U_F ranges from 86 $\mu\text{m}\cdot\text{s}^{-1}$ to 1300 $\mu\text{m}\cdot\text{s}^{-1}$ and is normalized with U_0. Color map represents the time fraction when flagellar beating is phase locked with external flow. It is equal to 1 (black) when phase locking is observed for the entire 30 s recording, while it is 0 (white) when phase locking is never observed. (b) Coupling strength ϵ as a function of external flow U_F/U_0.

$$\frac{\partial P}{\partial t} = \frac{\partial[\nu + \varepsilon \sin(2\pi\Delta)P]}{\partial\Delta} + T_{\text{eff}}\frac{\partial^2 P}{\partial\Delta^2}. \tag{2}$$

The Fokker-Planck Eq. (2) has a time-independent solution

$$\hat{P}(\Delta) = \frac{1}{C}\int_{\Delta}^{\Delta+1} \exp\left(\frac{V(\Delta') - V(\Delta)}{T_{\text{eff}}}\right) d\Delta', \tag{3}$$

where C is a normalization constant [33]. The solution (3) only depends on three parameters ν, ϵ, and T_{eff} and is computed numerically using the Gauss-Laguerre quadrature. For large $|\nu|$, $\hat{P}(\Delta)$ is uniform. When $|\nu|$ is decreased, the probability $\hat{P}(\Delta = 0)$ of in-phase beating increases, while the probability $\hat{P}(\Delta = \pm 0.5)$ of antiphase beating decreases. For small $|\nu|$, the phase is locked. $\hat{P}(\Delta)$ is Gaussian-like, with a zero probability to beat in antiphase; see Fig. 3.

We examine cell motility over a wide range of amplitudes $A_F = 0$–10 μm and frequencies $f_F = 43$–68 Hz, corresponding to $U_F = 0$–$1360 \mu\text{m}\cdot\text{s}^{-1}$. In comparison, we measure the free swimming velocity to be $U_0 = 110 \pm 12 \mu\text{m}\cdot\text{s}^{-1}$. Figure 4 presents our experimental data for 11 data sets and 171 separate recordings. Each data set corresponds to recordings of the same cell subject to flows of fixed A_F and different f_F. For low amplitude forcing, $U_F \approx 100$ $\mu\text{m}\cdot\text{s}^{-1}$, phase locking is never observed, regardless of how close f_F is from f_0. For $U_F \geq 250$ $\mu\text{m}\cdot\text{s}^{-1}$, synchronization transitions similar to the ones in Figs. 2–3 are observed for all data sets.

The size of the synchronization region characterizes the synchronization force and is determined by fitting experimental phase distributions with the solution (3) of Eq. (2). $\hat{P}(\Delta)$ depends on $\nu = f_F - f_0$, T_{eff}, and ϵ. The noise level T_{eff} stems from stochasticity in the flagellar actuation and is assumed to be a cell-dependent constant. We assume the external forcing ϵ to scale directly with the hydrodynamic force on the flagella and hence to be linear in the flow velocity, $\epsilon \sim U_F$. Within a data set, A_F is constant and we

write $\epsilon = \epsilon_0 f_F/f_0$. Hence, $\hat{P}(\Delta)$ depends on f_0, ϵ_0, and T_{eff}, which are determined by least-squares fitting. Figure 3 shows the agreement between the distribution of phase differences for the data set detailed in Figs. 2–3 and the computed $\hat{P}(\Delta)$. We compute the average beating frequency predicted by Eq. (1) as

$$f = \int_0^1 -\frac{dV}{d\Delta}\hat{P}(\Delta)d\Delta. \quad (4)$$

Experimental measurements of f agree with Eq. (4); see Fig. 2(c). At the synchronization transition, the square root behavior of f carries the characteristic signature of a saddle-node bifurcation. These results confirm that the stochastic phase dynamics is accurately represented with only three parameters f_0, T_{eff}, and ϵ_0.

The fitting procedure is repeated for each data set and ϵ is measured for a wide range of flow conditions. The values for f_0 and T_{eff} are consistent between cells with $f_0 = 52.6 \pm 1.1$ Hz and $T_{\text{eff}}/f_0 = 0.0008 \pm 0.0003$. Our measurements of T_{eff} agree with previously reported values [10,34]. We find ϵ to increase linearly with U_F and directly measure ϵ as a function of the hydrodynamic forces $\epsilon = \mu U_F/U_0$ with $\mu = 0.51\ \text{s}^{-1}$; see Fig. 4(b). This result agrees with the shape of an Arnold tongue, the prototypical synchronization region of the model system (1); see Fig. 4(a).

Discussion.—Recent work established synchronization through hydrodynamic interactions between two isolated flagella of Volvox, whose intrinsic beating frequencies differed by ~10% [14]. Volvox and *C. reinhardtii* are different organisms and the synchronization modes observed in Ref. [14] are different from the symmetric breaststroke of wt *C. reinhardtii* investigated here. Our experiments demonstrate that eukaryotic flagella respond to hydrodynamic forces and can be synchronized with an external flow. For *C. reinhardtii*, interflagellar synchronization requires phase-locking between two flagella, whose intrinsic beating frequencies differ by as much as 30%, hence, requiring coupling strengths $\epsilon \approx 15$–20 Hz [35]. In contrast, in our experiments for $U_F \approx 10U_0$, the hydrodynamic forces on the flagella are an order of magnitude larger than those experienced for free-swimming cells, yet the flagella only synchronize to flows with forcing frequencies within 5 Hz of f_0. From Fig. 4(b), synchronization at 15–20 Hz from f_0 would require flows of over $30U_0 \approx 3300\ \mu\text{m.s}^{-1}$.

Furthermore, for the largest flows $U_F \approx 10U_0$ when f_F is outside of the synchronization region, the velocity field around the cell due to the background flow is 10–100 times larger than the flow field due to hydrodynamic interactions, see numerical calculations in the Supplemental Material [26]. However, the flagella do not synchronize to the background flow but do remain synchronized to each other and perform symmetrical breaststrokes. In wt *C. reinhardtii* performing breaststrokes, it seems unlikely that interflagellar synchronization is due to hydrodynamic interactions, since the velocity field is dominated by the background flow to which the two flagella are not synchronized. Our results suggest that interflagellar synchronization does not primarily involve external hydrodynamic forces and point instead towards a cell-internal synchronization mechanism.

Scanning electron micrographs (SEMs) of the region around the basal bodies from which the flagella emerge reveal that a ~200 nm long contractile fiber, the distal striated fiber, mechanically connects the basal bodies of the two flagella [36]. It appears most plausible that this mechanical connection through the distal striated fiber plays a major role in flagellar synchronization for *C. reinhardtii*, also discussed in Refs. [22,23]. Indeed, if we consider a force balance on one flagellum, the total hydrodynamic force exerted by the flagellum on the surrounding fluid is exactly balanced by the direct mechanical force the same flagellum exerts on the basal apparatus. As a result, strong mechanical stress concentration is expected in the region of the cell cortex around the basal apparatus of the flagella, which far exceeds the viscous stresses inside the fluid. Synchronization is therefore more likely mediated by elastic stresses, which are conservative and act over an interflagellar distance of only ~200 nm in the distal fiber, rather than viscous stresses, which are dissipative and act over an interflagellar distance of ~10 μm in the fluid.

To test this hypothesis, we investigated the mutant *vfl3* of *C. reinhardtii*. SEMs of *vfl3* cells have revealed defects in the distal striated fiber [24,37], which mechanically connects the flagella. Using the same experimental setup, we observed the motility of 20 biflagellated *vfl3* cells. Each individual flagellum of *vfl3* beats actively with normal waveforms and frequencies. However, for this mutant with impaired mechanical connection, the two flagella are always observed to beat in asynchronous fashion for the entire duration of the recordings, with no frequency locking recorded in flagellar beating, except in one cell where periods of phase locking were recorded. For most cells, the two flagella beat in the same direction, in contrast with wt cells, whose flagella beat in opposite direction when performing a breaststroke; see also Ref. [24]. For *vfl3* cells, we found the slower flagellum to beat at 48.6 ± 8.8 Hz and the faster one at 63.1 ± 6.9 Hz. These observations are consistent with a synchronization mechanism relying on the distal striated fiber, since for the mutant *vfl3* with an impaired mechanical connection between the flagella, the *cis* and the *trans* flagellum beat at their own intrinsic frequency.

These experiments for *C. reinhardtii* highlight the role of elastic stresses in the cell cortex for flagellar synchronization and have wide implications for ciliates. Contractile fibers connecting flagella and cilia are found across organisms [21]. In particular, for multiciliated cells, the network of elastic actin fibers connecting dozens of cilia was reported to play a role in coordination of ciliary beating [38,39]. Perturbing the bridges between these actin fibers resulted in

loss of metachronal synchrony of cilia beating [38]. Further investigation in other ciliated organisms is needed to assess the prevalence of such intracellular coupling. The role of the striated fibers is currently investigated for *C. reinhardtii*.

We thank Jerry Westerweel for useful conversations, and Roland Kieffer, Vinesh Badloe, and Edwin Overmars for their help in setting up the experiment. The work has been supported by a TU Delft Technology Fellowship and a Marie Curie CIG Grant (No. 618454).

*m.e.aubin-tam@tudelft.nl
†d.s.w.tam@tudelft.nl

[1] T. Vicsek, Nature (London) **411**, 421 (2001).
[2] S. H. Strogatz, Physica (Amsterdam) **143D**, 1 (2000).
[3] T. Niedermayer, B. Eckhardt, and P. Lenz, Chaos **18**, 037128 (2008).
[4] B. Guirao and J.-F. Joanny, Biophys. J. **92**, 1900 (2007).
[5] S. Gueron, K. Levit-Gurevich, N. Liron, and J. J. Blum, Proc. Natl. Acad. Sci. U.S.A. **94**, 6001 (1997).
[6] R. Golestanian, J. M. Yeomans, and N. Uchida, Soft Matter **7**, 3074 (2011).
[7] M. Polin, I. Tuval, K. Drescher, J. P. Gollub, and R. E. Goldstein, Science **325**, 487 (2009).
[8] G. Taylor, Proc. Math. Phys. Eng. Sci. **209**, 447 (1951).
[9] K. C. Leptos, K. Y. Wan, M. Polin, I. Tuval, A. I. Pesci, and R. E. Goldstein, Phys. Rev. Lett. **111**, 158101 (2013).
[10] R. E. Goldstein, M. Polin, and I. Tuval, Phys. Rev. Lett. **103**, 168103 (2009).
[11] U. Rüffer and W. Nultsch, Cell Motil. **5**, 251 (1985).
[12] R. R. Bennett and R. Golestanian, Phys. Rev. Lett. **110**, 148102 (2013).
[13] A. Vilfan and F. Jülicher, Phys. Rev. Lett. **96**, 058102 (2006).
[14] D. R. Brumley, K. Y. Wan, M. Polin, and R. E. Goldstein, eLife **3**, e02750 (2014).
[15] R. E. Goldstein, M. Polin, and I. Tuval, Phys. Rev. Lett. **107**, 148103 (2011).
[16] V. F. Geyer, F. Jülicher, J. Howard, and B. M. Friedrich, Proc. Natl. Acad. Sci. U.S.A. **110**, 18058 (2013).
[17] B. M. Friedrich and F. Jülicher, Phys. Rev. Lett. **109**, 138102 (2012).
[18] L. Fredrickson-Hemsing, S. Ji, R. Bruinsma, and D. Bozovic, Phys. Rev. E **86**, 021915 (2012).
[19] C. Shingyoji, I. R. Gibbons, A. Murakami, and K. Takahashi, J. Exp. Biol. **156**, 63 (1991).
[20] I. Gibbons, C. Shingyoji, A. Murakami, and K. Takahashi, Nature (London) **325**, 351 (1987).
[21] M. Sleigh, Nature (London) **277**, 263 (1979).
[22] D. L. Ringo, J. Cell Biol. **33**, 543 (1967).
[23] J. S. Hyams and G. G. Borisy, Science **189**, 891 (1975).
[24] H. J. Hoops, R. L. Wright, J. W. Jarvik, and G. B. Witman, J. Cell Biol. **98**, 818 (1984).
[25] E. Harris, *The Chlamydomonas Sourcebook* (Elsevier Science, 2009), Vols. 1 and 3.
[26] See Supplemental Material http://link.aps.org/supplemental/10.1103/PhysRevLett.115.238101 for a description of the numerical calculations, which compare the flow velocity field generated by one flagellum and the flow velocity field generated by the motion of the piezostage, which includes Refs. [27–30].
[27] H. Power and G. Miranda, SIAM J. Appl. Math. **47**, 689 (1987).
[28] P.-O. Persson and G. Strang, SIAM Rev. **46**, 329 (2004).
[29] K. Drescher, R. E. Goldstein, N. Michel, M. Polin, and I. Tuval, Phys. Rev. Lett. **105**, 168101 (2010).
[30] H. Kurtuldu, D. Tam, A. E. Hosoi, K. A. Johnson, and J. P. Gollub, Phys. Rev. E **88**, 013015 (2013).
[31] L. Cohen, *Time-Frequency Analysis* (Prentice hall, 1995), Vol. 1.
[32] K. Y. Wan and R. E. Goldstein, Phys. Rev. Lett. **113**, 238103 (2014).
[33] A. Pikovsky, M. Rosenblum, and J. Kurths, *Synchronization: A Universal Concept in Nonlinear Sciences* (Cambridge University Press, Cambridge, England, 2003), Vol. 12.
[34] R. Ma, G. S. Klindt, I. H. Riedel-Kruse, F. Jülicher, and B. M. Friedrich, Phys. Rev. Lett. **113**, 048101 (2014).
[35] U. Rüffer and W. Nultsch, Cell Motil. **7**, 87 (1987).
[36] C. D. Silflow and P. A. Lefebvre, Plant Physiol. **127**, 1500 (2001).
[37] R. L. Wright, B. Chojnacki, and J. W. Jarvik, J. Cell Biol. **96**, 1697 (1983).
[38] M. E. Werner, P. Hwang, F. Huisman, P. Taborek, C. Y. Clare, and B. J. Mitchell, J. Cell Biol. **195**, 19 (2011).
[39] E. R. Brooks and J. B. Wallingford, Curr. Biol. **24**, R973 (2014).